Published by Institute of Physics Publishing for SISSA

Received: *January 12, 2007*
Revised: *June 14, 2007*
Accepted: *August 3, 2007*
Published: *August 28, 2007*

LHC signals of T-odd heavy quarks in the Littlest Higgs model

Debajyoti Choudhury and Dilip Kumar Ghosh

Department of Physics & Astrophysics,
University of Delhi, Delhi-110007, India
E-mail: debchou@physics.du.ac.in, dkghosh@physics.du.ac.in

Abstract: Recently proposed Little Higgs models present a viable solution to the naturalness problem of the Standard Model. An additional discrete symmetry, called T-parity, has been included in the simplest Little Higgs models to evade the constraints arising from electroweak precision data. The Littlest Higgs model with T-parity (LHT) not only predicts a set of new fermions in addition to the heavy gauge bosons of the original Little Higgs model, but also provides a new candidate for dark matter. In this paper, we study two particularly interesting signatures of T-odd fermion pair production at the LHC, namely, (*a*) $jj + \ell^+\ell^- + \not{E}_T$ and (*b*) $jj + b\bar{b} + \ell^\pm + \not{E}_T$. Using a parton level Monte Carlo event generator, we evaluate both the signal as well as the standard model background profile for a selected set of model parameters thereby developing a good discriminator. Finally, we scan the parameter space and delineate the possible discovery region in the same.

Keywords: Spontaneous Symmetry Breaking, Beyond Standard Model, Gauge Symmetry, Global Symmetries.

JHEP08(2007)084

Contents

1. Introduction **1**

2. The model **3**

3. The 1st and 2nd generation T-odd heavy quark production and decay **4**

4. Signal and background analysis **6**

4.1 $pp \to Q_H\bar{Q}_H \to q'\bar{q}' + W_H^+W_H^- \to jj + \ell^+\ell^- + \not{E}_T$ 7

4.2 $pp \to Q_H\bar{Q}_H \to q'\bar{q} + W_H^\pm Z_H \to jj + b\bar{b} + \ell^\pm + \not{E}_T$ 10

5. Discovery limit **13**

6. Conclusions **14**

1. Introduction

The experimental observation of the Higgs boson(s) and the determination of its (their) properties is crucial for the understanding of Electro-Weak Symmetry Breaking (EWSB) and hence constitutes one the major goals of the presently operating high energy collider viz. the Tevatron (Run II) as well as future ones such as the forthcoming LHC and the planned International Linear Collider (ILC). This process is rendered even more complicated by the fact that within the Standard Model (SM), the Higgs boson mass is not predicted uniquely. Negative results from current search efforts, thus, serve only to set a lower bound of 114 GeV on its mass [1, 2]. Precision electroweak data, on the other hand, favor a light Higgs boson with a mass $m_H \leq 186$ GeV at 95% CL [3].

This immediately leads us to the fine-tuning problem in the SM, namely that there is no symmetry which can protect the Higgs mass M_h from large radiative corrections from the ultra-violet. As this constitutes an outstanding theoretical problem with the SM, several mechanisms to protect the Higgs mass have been proposed; examples include technicolor, supersymmetry and a low fundamental quantum gravity scale. Of these, supersymmetry is especially popular as the stabilization of M_h is assured in a *natural manner* due to the symmetry between the bosonic and fermionic degrees of freedom in the theory. On the other hand, technicolor theories solve the hierarchy problem by introducing some strong interactions at scales not too much above the electroweak scale. The low scale fundamental quantum gravity models resolve the issue by just lowering the fundamental Planck scale. Unfortunately though, despite intensive efforts over decades, no experimental hint for any of these scenarios has been forthcoming. Consequently, it is very important to explore alternative mechanisms for EWSB that are testable in current or forthcoming experiments.

JHEP08(2007)084

Recently, such an alternative mechanism for solving the naturalness problem of the standard model has been developed [4]. Dubbed as Little Higgs models, these incorporate the SM Higgs as a pseudo-Goldstone boson of some global symmetry which is spontaneously broken at a high scale $\Lambda(\equiv 4\pi f) \sim 10\,\text{TeV}$. The low energy effective theory is described by a non-linear sigma model. With the introduction of new gauge bosons and partners of the top quark with masses of the order of f, the quadratically divergent contributions to the Higgs mass are exactly cancelled at the one loop level, thereby ameliorating the fine-tuning problem.

However, in the presence of such a plethora of new particles, the electroweak observables receive additional contributions at the tree level due to the exchange of heavy gauge bosons (as also from a non-zero vacuum expectation of a triplet Higgs field that often comes about naturally). These additional contributions are in direct conflict with experimental data, unless the scale f is above $\sim 5\,\text{TeV}$ [5]. For such a large value of f, one faces the re-introduction of a fine tuning between the cutoff scale ($\sim 4\pi f$) for the model and the weak scale. To circumvent this serious problem of the original Little Higgs model, a new discrete symmetry, called T-parity (and analogous to the R parity in the MSSM), has been introduced. The Littlest Higgs Model with T-parity (LHT) [6 – 9] provides a fully realistic and consistent model which satisfies the electroweak precision data. Under this new symmetry all standard model fields are T-even, while the new heavy partners are T-odd. As a consequence, all T-odd fields can only be generated in pairs. Furthermore, after the electroweak symmetry breaking, mixing between standard model gauge bosons with their T-odd counterparts is prohibited by this new discrete symmetry. Hence, there are no tree level contributions from T-odd heavy partners of the standard model particles to the electroweak precision observables. With all such corrections arising only at the one loop level or beyond, these are naturally small. As a result of this, the electroweak precision data now allows for a relatively low value of new particle mass scale $f \sim 500\,\text{GeV}$ [8], thereby leading to copious production of different T-odd heavy partners of the standard model particles at the LHC as well as future e^+e^- linear collider (ILC) [7, 10 – 13]. Another interesting feature of T-parity is the existence of a neutral and colorless weakly interacting stable T-odd particle (LTP) A_H, the heavy partner of the hypercharge gauge boson; very often termed the *heavy photon*, it is a good candidate for cold dark matter [14].

The long waited pp Large Hadron Collider (LHC), to be operative in a year from now, will be of great importance in revealing the mystery of the electroweak symmetry breaking. While the major thrust would be on the discovery of the standard model Higgs, it will also provide a great opportunity to explore alternate mechanisms of the electroweak symmetry breaking. This has motivated some phenomenological studies of the Littlest Higgs model with T-parity [10 – 13, 15]. In this paper, we revisit the LHC signatures of the first two generation T-odd heavy quark pair production within the Littlest Higgs model(LHT) [11, 10, 12]. Performing a detailed estimation of the observability of two type of signals (a) $jj + \ell^+\ell^- + \not{E}_T$ and (b) $jj + b\bar{b} + \ell^\pm + \not{E}_T$, we provide the discovery region at the LHC of the LHT parameter space. The rest of the paper is organized as follows. In section 2, we briefly discuss the main features of the model. In section 3, we discuss pair production of T-odd heavy quarks and its two body decay branching ratio into standard

JHEP08(2007)084

model quarks and T-odd heavy gauge bosons. In section 4, signal and background events are discussed in detail. In section 5, we discuss the possible 5σ discovery region in the LHT parameter space using the signal (b). Finally, our conclusions are given in section 6.

2. The model

The Littlest Higgs model with T-parity has been studied in great detail elsewhere [6 – 8], and here we briefly discuss some important features of the model relevant for our analysis. It is a non-linear sigma model based on a SU(5) global symmetry of which a $[\mathrm{SU}(2)_1 \times \mathrm{U}(1)_1] \times [\mathrm{SU}(2)_2 \times \mathrm{U}(1)_2]$ subgroup is gauged. A discrete symmetry (T-parity), exchanging the two $[\mathrm{SU}(2) \times \mathrm{U}(1)]$ groups is naturally introduced in the model. At a scale f, the global symmetry is spontaneously broken down to a SO(5) group resulting in 14 massless Nambu-Goldstone (NG) bosons [4]. Simultaneously, the gauged symmetry is broken down to its subgroup $\mathrm{SU}(2)_L \times \mathrm{U}(1)_\mathrm{Y}$ identified as the standard model gauge group. Consequently, of the 14 NG bosons, four are eaten by the heavy gauge bosons associated with the broken symmetry. The remaining NG bosons decompose into a T-even SU(2) doublet h, considered to be the standard model Higgs doublet, and a complex T-odd SU(2) triplet Φ, which acquires a mass $M_\Phi = \sqrt{2} M_h f / v_\mathrm{SM}$ at one loop, with M_h being the standard model Higgs mass. These Higgs bosons remain in the low energy effective theory.

After electroweak symmetry breaking, the masses of the T-odd heavy partners of the photon (A_H), Z-boson (Z_H) and W-boson(W_H) are given by

$$\begin{aligned} M_{A_H} &\simeq \frac{g' f}{\sqrt{5}} \left[1 - \frac{5 v_\mathrm{SM}^2}{8 f^2} + \ldots \right] ; \\ M_{Z_H} \simeq M_{W_H} &= g f \left[1 - \frac{5 v_\mathrm{SM}^2}{8 f^2} + \ldots \right] . \end{aligned} \tag{2.1}$$

Here, $v_\mathrm{SM} \simeq 246\,\mathrm{GeV}$ is the electroweak symmetry breaking scale. Since $g' < g$, A_H is substantially lighter than other T-odd heavy gauge bosons.

For consistent implementation of T-parity in the fermion sector, each standard model fermion doublet must be replaced by a pair of fields $F_\alpha (\alpha = 1, 2)$ [6 – 8], where each F_α is a doublet under $\mathrm{SU}(2)_\alpha$ and singlet under the other. The aforementioned T-parity exchanges F_1 and F_2. The T-even combination of F_α is identified with the standard model fermion doublet and the other (T-odd) combination is its heavy partner (F_H). To generate mass terms for these T-odd heavy fermions through Yukawa interactions one requires additional T-odd SU(2) singlet fermions in the theory as suggested in [6 – 8]. Assuming universal and flavour diagonal Yukawa couplings κ [1] we have, for U_H and D_H (the T-odd heavy partners of the standard model quarks (u, c) and (d, s) respectively),

$$M_{D_H} \simeq \sqrt{2}\, \kappa\, f\,, \qquad M_{U_H} \simeq \sqrt{2}\, \kappa\, f \left(1 - \frac{v_\mathrm{SM}^2}{8\, f^2} \right) . \tag{2.2}$$

[1] Non universal Yukawa couplings may lead to potentially large flavour changing neutral current effects, studied in refs. [16, 17].

Since $f \gtrsim 500\,\text{GeV}$, it is clear from eq. (2.2) that the up and down type T-odd heavy partners have nearly equal masses. We will not discuss the top sector of the model, since in this paper our main focus will be on the first two generation heavy quarks. Further details about the implementation of T-parity in the fermion sector including the top quark sector can be found in refs. [6 – 8, 11]. In summary, the complete spectrum of the Littlest Higgs model(LHT) with T-parity relevant for our analysis will only depend on two free parameters: the new physics scale f and the flavour independent Yukawa coupling κ whose range is $0.5 \leq \kappa \leq 1.5$ [7, 8].

3. The 1st and 2nd generation T-odd heavy quark production and decay

Based on the model of section 2, we now calculate the leading order production rates of T-odd quarks at the LHC. The latter can be copiously pair produced ($Q_H\bar{Q}_H$) as long as their masses are not too large. With the dominant production mechanism being the QCD one (both $q\bar{q}$ and gg initiated), one may safely neglect the sub-dominant weak production amplitudes. In fact, the latter contributions to $Q_H\bar{Q}_H$ production are even smaller than those leading to electroweak processes such as $uu \to UU$ or $dd \to DD$. Although the last-mentioned lead to interesting final states containing like-sign dilepton pairs, we choose to neglect these.in the current analysis.

As the heavy quarks corresponding to the first two generations are nearly degenerate, and lead to very similar final state configurations, we sum over all four flavours. In our numerical analysis, we use the CTEQ5L parton distribution functions [18]. Variation of the factorisation scale over the range $m^2_{Q_H}/4 < Q^2 < 4m^2_{Q_H}$ corroborates the naive expectation of the signal cross-section falling off with an increase in the scale, and, to be conservative, we choose $Q^2 = 4m^2_{Q_H}$. In figure 1, we display the production rate of the T-odd quark as a function of the scale f for three values of the parameter κ namely $\kappa = 0.6, 1$ and 1.5.

Although the production cross section depends only on the mass of the heavy quark, and thus on the product κf, both the branching fractions as well as the decay distributions have additional dependence on the scale f and hence we choose to display the three curves in figure 1 so as to facilitate future comparisons.

Once these heavy T-odd quarks are produced, they will promptly decay into (T-even) standard model quarks and T-odd heavy gauge bosons $(W^{\pm}_H, Z_H, A_H)$[2]. Now, as we have indicated in section 2, the masses of the latter are functions only of f. As a comparison of eq. (2.2) with eqs. (2.1) shows, U_H and D_H are always significantly heavier than the T-odd gauge bosons, with a slightest hint of phase suppression in $Q_H \to q + Z_H\,(q' + W_H)$ appearing only for the smallest allowed values for κ. More importantly, the $Q_H q^{(\prime)} V_H$ couplings too depend on f. Whereas the couplings $U_H - d - W_H$ and $D_H - u - W_H$ are of equal strength owing to SU(2) invariance of the Lagrangian,

$$g_{U_H d W_H} = g_{D_H u W_H} = g/\sqrt{2}\,,$$

[2]In our analysis, we focus on the region of the parameter space where the T-odd quarks are heavier than the T-odd gauge bosons. For the complementary region, the search strategy would have to be a different one.

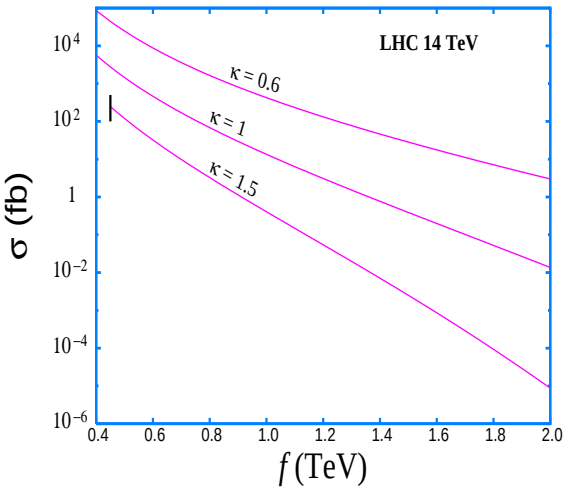

Figure 1: The variation of the leading order T-odd quark pair $(U_H\bar{U}_H + D_H\bar{D}_H + C_H\bar{C}_H + S_H\bar{S}_H)$ production with the scale f for $\kappa = 0.6, 1$ and 1.5. The curve corresponding to $\kappa = 1.5$, starts only from $f = 450\,\text{GeV}$, which is the minimum value required to satisfy the bound on the T-odd heavy quark mass $M_{Q_H} < 4.8\left(\frac{f}{1\ \text{TeV}}\right)^2$ TeV [8].

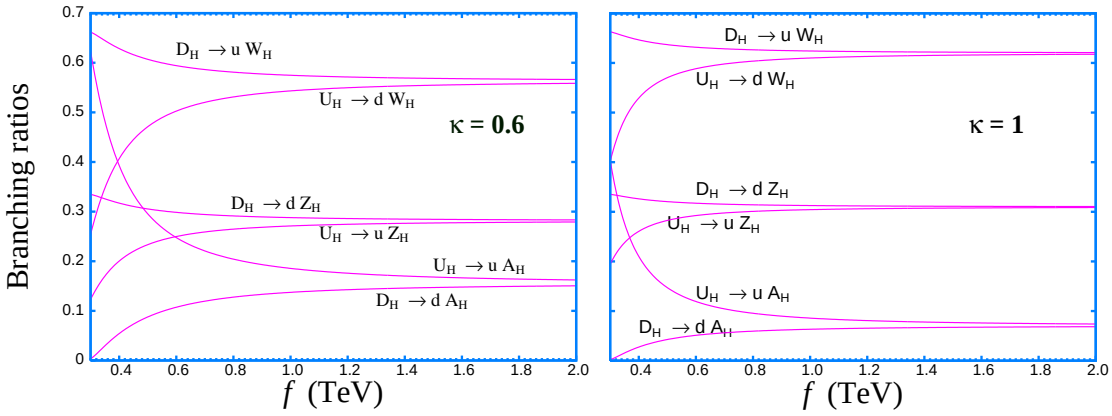

Figure 2: Variation of the decay branching ratio of heavy Quarks in the LHT model with the scale f for two values of the parameter $\kappa = 0.6$ (left panel) and 1 (right panel).

the couplings to the Z_H and A_H have a crucial dependence on isospin (T_3), namely

$$g_{f_H f Z_H} = g\, c_H\, T_{3f} + g'\, s_H\, Y'\,, \qquad g_{f_H f A_H} = -g\, s_H\, T_{3f} + g'\, c_H\, Y'\,,$$

where $Y' = -1/10$ and θ_H is the Weinberg angle in the heavy sector:

$$s_H \equiv \sin\theta_H \simeq \frac{5\, g\, g'}{5\, g^2 - g'^2}\, \frac{v_{\rm SM}^2}{4\, f^2}\,, \qquad c_H \equiv \cos\theta_H\ .$$

This immediately opens up the possibility for a cancellation in $g_{D_H dA_H}$ for a relatively small f, and consequently in the suppression of $\Gamma(D_H \to d + A_H)$ for small f. This, for example, is reflected in figure 2 where we display the variation of the two body decay branching ratios of the T-odd quarks into standard model quarks and heavy T-odd gauge bosons as a function of the scale f.

4. Signal and background analysis

In this section, we discuss the LHT signal arising from the production and decay of heavy T-odd quarks of first two generations. We also discuss possible standard model backgrounds and elaborate on the selection criteria necessary for such signals to be significantly observed over the standard model background. The large number of diagrams contributing to the standard model background are calculated using the helicity amplitude package MADGRAPH [19]. To estimate the number of signal and background events as well as their phase space distribution(s), we use a parton level Monte-Carlo event generator. As *acceptance criteria* for both the signal and background events we use the following initial set of cuts:

(i) We require that both jets and leptons should appear within the detectors' rapidity coverage, namely

$$| \eta(\ell, j) | < 2.5 \ . \tag{4.1}$$

(ii) The leptons and jets should have energy large enough to render them visible to the detector. Imposing this in terms of transverse momenta, we demand that

$$p_T^{\rm jets} > 30 \text{ GeV} , \qquad p_T^{\ell} > 20 \text{ GeV} \ . \tag{4.2}$$

(iii) Finally, we must also ensure that the jets and leptons are well separated so that they can be identified as individual entities. For this, we use the well-known cone algorithm defined in terms of a cone angle $\Delta R_{\alpha\beta} \equiv \sqrt{(\Delta\phi_{\alpha\beta})^2 + (\Delta\eta_{\alpha\beta})^2}$ with $\Delta\phi$ and $\Delta\eta$ being the azimuthal angular separation and rapidity difference between two particles. We demand that

$$\Delta R_{jj} > 0.7 , \quad \Delta R_{\ell j} > 0.4 , \quad \Delta R_{\ell\ell} > 0.3 \ . \tag{4.3}$$

While some of the above might seem too harsh as acceptance criteria, it should be realized that simulating an actual detector environment would typically necessitate further refinements and that the requirements of eqs. (4.1)–(4.3) are to be treated more as robust guidelines. Indeed, harsher requirement on jet rapidity or transverse momenta would suppress the QCD background events (wherein jets come from initial or final state radiation) without affecting the signal to any significant degree.

It stands to reason that finite resolution effects result in a difference between the energy as measured by the detector and its true value. To account for this in a realistic fashion,

LHT parameter set					
A			**B**		
$f = 1$ (TeV), $\kappa = 0.6$			$f = 1$ (TeV), $\kappa = 1.0$		
M_{Q_H} (GeV)	M_{V_H} (GeV)	M_{A_H} (GeV)	M_{Q_H} (GeV)	M_{V_H} (GeV)	M_{A_H} (GeV)
842	648	154	1404	648	154

Table 1: The LHT parameter set for the signal study. V_H corresponds to $W_H^\pm$ and Z_H.

Parameter set $\Rightarrow$	**A**	**B**	$\sigma_{\text{background}}$(fb)	
Cuts $\Downarrow$	$\sigma_{\text{sig.}}$(fb)	$\sigma_{\text{sig.}}$(fb)	$t\bar{t}$	W^+W^-jj
Acceptance	4.28	0.18	1095	204
$M_{jj} \notin [65, 105]$ GeV	4.19	0.18	892	168
$M_{\ell\ell} \notin [75, 105]$ GeV	3.92	0.17	714	136
$\not{E}_T > 200\,\text{GeV}$	2.48	0.17	5.6	9.33
$\not{E}_T > 300\,\text{GeV}$	1.40	0.13	0.65	3.12
$\not{E}_T > 400\,\text{GeV}$	0.62	0.10	0.10	1.16

Table 2: The effect of incremental increase of cuts on the signal and background rates (fb) for the process $pp \to Q_H\bar{Q}_H \to q\bar{q}W_H^+W_H^- \to jj + \ell^+\ell^- + \not{E}_T$. The LHT parameter sets **A** and **B** are defined in table 1.

we impose a Gaussian smearing on the measured energy with a width given by

$$\frac{\delta E_j}{E_j} = \left[\frac{(0.6)^2\text{GeV}}{E_j} + (0.04)^2\right]^{1/2}, \qquad \frac{\delta E_\ell}{E_\ell} = \left[\frac{(0.12)^2\text{GeV}}{E_\ell} + (0.01)^2\right]^{1/2}$$

respectively. All the cuts described above as well as any further selection criteria are to be imposed after smearing the energies as above. We may now discuss our strategies for the detection of T-odd heavy quarks at the LHC. For the purpose of contrasting the phase space distributions of signal and background events, we choose to work with two particular points in the parameter set as displayed in table 1.

The simplest final state would arise when both Q_H and $\bar{Q}_H$ would decay in the $(q+A_H)$ channel. However, the observed final state, namely dijet with missing transverse momentum is fraught with a very large SM background. In fact, most final state configurations arising as a result of even one of Q_H and $\bar{Q}_H$ decaying directly into $(q + A_H)$ suffer on this account. In view of such considerations, we concentrate on two particular modes as described below.

4.1 $pp \to Q_H\bar{Q}_H \to q'\bar{q}' + W_H^+W_H^- \to jj + \ell^+\ell^- + \not{E}_T$

This particular final state arises when both the T-odd heavy quarks decay into the $(q + W_H^\pm)$ mode (with a branching fraction as shown in figure 2). The T-odd gauge bosons $(W_H^\pm)$ decay into the standard model gauge boson $W^\pm$ and the LTP A_H with $\sim 100\%$ branching ratio. And finally, both the W's decay leptonically with total branching fraction of $\sim (2/9)^2$. The missing transverse energy $(\not{E}_T)$ is due to the presence of two heavy LTPs

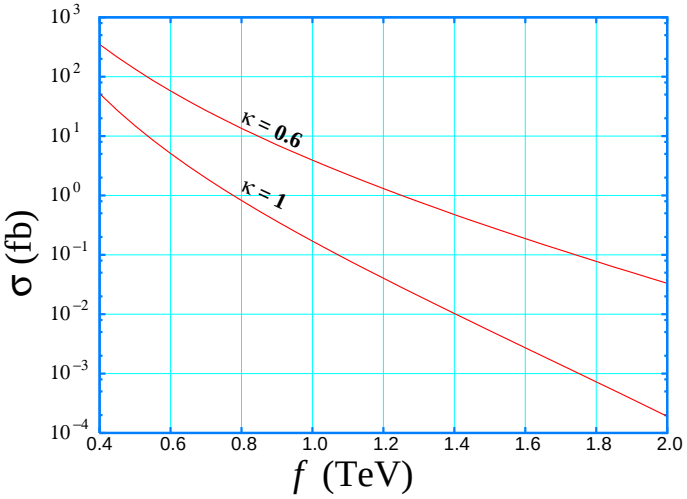

Figure 3: The variation of the signal ($pp \to Q_H\bar{Q}_H \to jj + \ell^+\ell^- + \not{E}_T$) cross-section with the scale f after imposing the acceptance criteria (eqs. 4.1)–(4.3) as well as the selection cut of eq. (4.4).

(A_H) and two neutrinos. For ease of detection, we discount τ's here and hence $\ell \equiv e, \mu$. And, while for the signal events the jets (j) are occasioned by hard processes involving two light quarks (u, d, s, c) in the final state, for the SM background one must also include hard gluon(s).

The major QCD-driven background to this signal emanates from the top pair production process $pp \to t\bar{t} \to b\bar{b}W^+W^- \to b\bar{b}\ell^-\ell^+\not{E}_T$ with both b-jets being misidentified as light quark jets. Here we assume that the mis-tagging probability of each b-jet as a non-b one is 40%. The second important source of background is the SM process $pp \to W^+W^-jj$, where both Ws decay leptonically and the two jets arise from either quarks or gluons (initial state radiation in the partonic subprocess).

In addition to W^+W^-jj, there are other electroweak processes contributing to the background, such as $ZZjj$, with one Z decaying into leptons and the other into neutrinos. Clearly, this background may be largely eliminated by requiring that the invariant mass of the lepton-pair be sufficiently away from M_Z. In an analogous fashion, the part of this same background wherein the jet-pair is a resultant of a W or Z decay, may be further reduced by stipulating that the dijet invariant mass not be close to either M_W or M_Z. In other words, our first selection cut (over and above the acceptance criteria) consists of

$$M_{jj} \notin [65, 105] \text{ GeV}\,, \qquad M_{\ell\ell} \notin [75, 105] \text{ GeV}\,. \tag{4.4}$$

Similar arguments also hold for other on-shell modes such as W^+W^-Z or $3\,W$'s. Of course, events wherein all the SM gauge bosons are off-shell escape this cut, but then these appear only at a very high order in perturbation theory and, consequently, are suppressed.

Clearly, the signal events are not expected to be affected seriously by the imposition of eq. (4.4), since the jets therein arise directly from Q_H decay, whereas the two leptons are the result of the decay of two different W's. By the same token, the $t\bar{t}$ as well as the

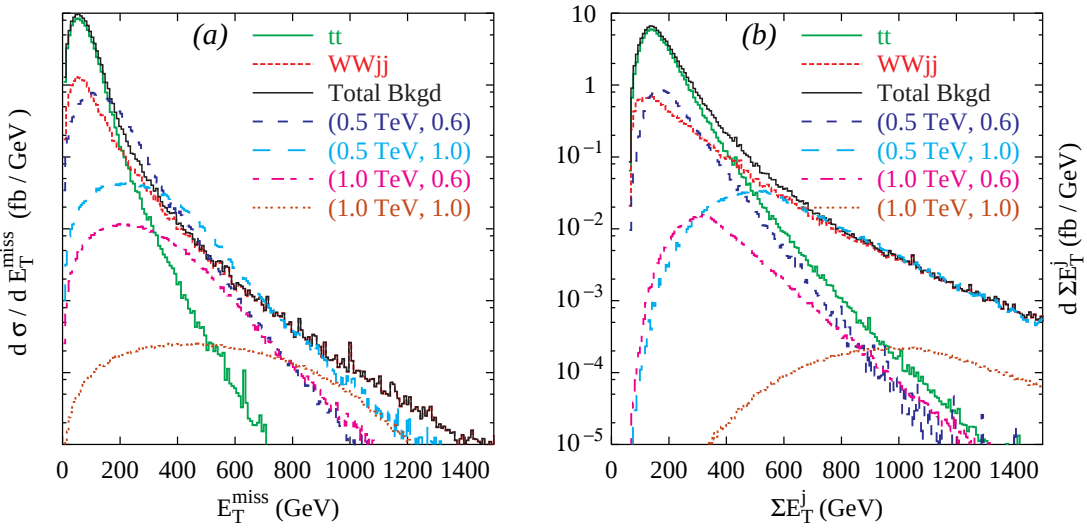

Figure 4: *(a)* Missing E_T distribution for the $jj\ell^+\ell^- + \not{E}_T$ final state. *(b)* Distribution in scalar sum of the jet transverse energies. Shown are the two dominant SM backgrounds as well as the signal for 4 representative points in the (f, κ) parameter space.

aforementioned W^+W^-jj background also largely escape this cut. This is illustrated by table 2, which displays the incremental effect of these two cuts on the major background as well as on the signal (for two particular points in the parameter space). Of course, the effect of the selection cut (as well as the acceptance criteria) on the signal cross section would depend on the masses of the T-odd quark and gauge bosons, and can be inferred from a comparison of the total cross sections (figure 1) with the post-cut effective cross-sections displayed in figure 3.

As is evinced from table 2, the number of $t\bar{t}$ and W^+W^-jj background events which survive eq. (4.4) are still orders of magnitude higher than the typical signal event rates. Thus, additional selection criteria are called for. An examination of the phase space distributions shows that missing transverse energy ($\not{E}_T$) is a very good discriminatory variable. This is not unexpected as the $\not{E}_T$ in the background events arises mainly from the two neutrinos, each of which come from the decay of a W and hence would typically have a transverse momentum of the order of m_W or smaller. The signal events, on the other hand, have, apart from the two neutrinos, two A_H's each of which are the decay products of a very heavy particle. In figure 4, we show the differential cross sections corresponding to the two major backgrounds as well as the signal (4 particular points in the parameter space).

It is immediately apparent that imposing a strong requirement on $\not{E}_T$ would result in a significant improvement in the signal to noise ratio. In table 2, we illustrate this for three choices of $\not{E}_T^{\rm min}$. A second variable of some interest is the scalar sum of the transverse energies of the two jets. Although it is not as discriminatory as $\not{E}_T$, it can be of importance in estimating the masses of the quarks and the gauge bosons if a signal is observed.

JHEP08(2007)084

4.2 $pp \to Q_H\bar{Q}_H \to q'\bar{q} + W_H^\pm Z_H \to jj + b\bar{b} + \ell^\pm + \not{E}_T$

This final state arises when one of the T-odd heavy quarks decays into $q + W_H^\pm$ mode, while the other one decays into $q + Z_H$ (the third mode, viz. $Q_H \to q + A_H$ can be dominant only for small f and that too just for the up-type quarks alone). Each of the gauge bosons undergoes a two-body decay to a LTP and a SM boson, viz. $W_H^\pm \to W^\pm + A_H$ and $Z_H \to h + A_H$, with nearly 100% branching ratio. And, in the final stages of the cascade, we consider only the leptonic decay of the W (branching fraction of $\sim 2/9$), whereas for the SM Higgs, with an assumed mass of $M_h = 120\,\text{GeV}$, we consider the dominant decay mode, viz. $b\bar{b}$ (branching fraction of 0.68).

The collider signature is an interesting one and consists of an isolated hard lepton ($\ell^\pm$), four well separated jets and a large missing transverse momentum, which owes itself to the presence of two heavy LTPs (A_H) and a neutrino from W decay. Furthermore, of the four jets, two would be tagged as b-jets. We assume here that the efficiency for tagging an individual b-jet is $\epsilon_b = 0.6$.

The major background to this particular channel comes from the following standard model processes:

- Top pair production with one top decaying hadronically and the other leptonically: $pp \to t\bar{t} \to b\bar{b}W^+W^- \to b\bar{b}jj\ell^\pm\not{E}_T$.
- $pp \to W^+hjj \to b\bar{b}jj + \ell^\pm\not{E}_T$, where the W decays leptonically and h decays into pair of b-jets, while the light quark jets originate mainly from initial state radiation.
- $pp \to W^\pm Zjj \to b\bar{b}jj + \ell^\pm\not{E}_T$, where W decays leptonically and Z decays into pair of b-jets. Again, the light quark jets are associated with initial state radiation.

On imposition of just the acceptance criteria (eqs. (4.1)–(4.3)), the signal cross-section is 2.08 fb and 0.077 fb for LHT parameter sets **A** and **B** respectively, whereas the background arising from top pair production is 8930 fb as can be seen from table 3. Clearly, some additional cuts are demanded, especially to remove the $t\bar{t}$ background, without suppressing the signal cross section. The first such selection criterion is exactly the one imposed in the previous subsection, namely that the invariant mass of the non-b dijet pair should not be too close to M_W or M_Z. In other words, that

$$M_{jj} \notin [65, 105] \ \text{GeV}. \tag{4.5}$$

This, clearly, would help eliminate the bulk of the $t\bar{t}$ background (see figure 5). In fact, the reduction factor is as large as 100 whereas the signal is hardly affected. Also eliminated would be the resonant contributions to the second and third backgrounds listed above, i.e those where the jj pair resulted from the decay of a gauge boson (WWh and WZh for the second; WWZ, WZZ for the third)[3]

Similarly, since the signal events correspond to the b-jets arising from the decay of Higgs, we demand that

$$| M_{b\bar{b}} - M_h | < 30 \ \text{GeV}. \tag{4.6}$$

[3]Since these are much smaller than the $t\bar{t}$ background (as well as other QCD contributions), we do not list them separately, although we do include these in our analysis.

JHEP08(2007)084

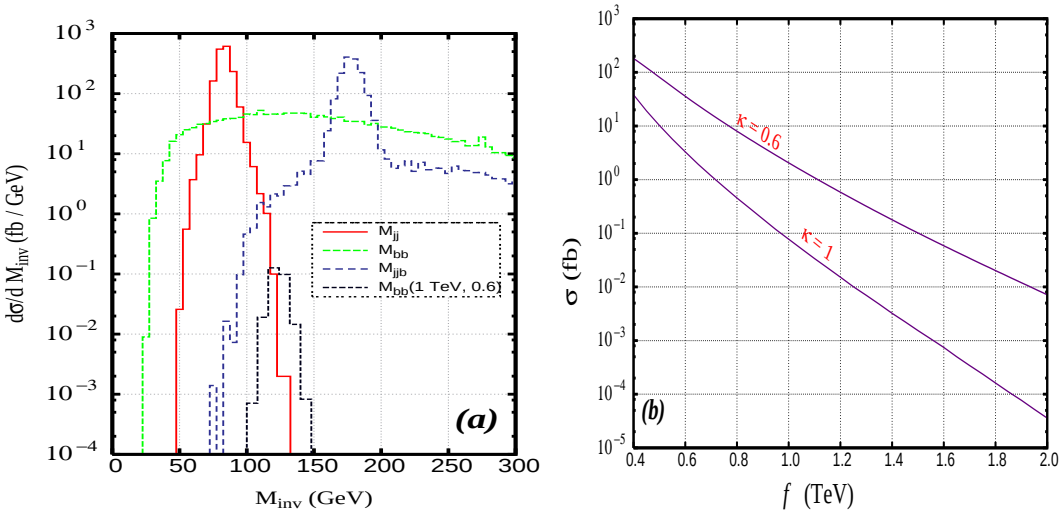

Figure 5: *(a)* $M_{jj}, M_{b\bar{b}}$ and M_{jjb} distributions for the standard model background to the $(jj + b\bar{b} + \ell^{\pm} + \not{E}_T)$ final state arising from $t\bar{t}$ production. For comparison, $M_{b\bar{b}}$ distribution for the signal ($f = 1\,\text{TeV}$ and $\kappa = 0.6$) process is also given. Only the selection cuts (eqs. (4.1)–(4.3)) have been applied and the b-tagging efficiency included. *(b)* The variation of the signal cross-section with the scale f, on imposition of the acceptance cuts (eqs. (4.1)–(4.3)) as well as the selection cuts of eqs. (4.5)–(4.8).

The $t\bar{t}$ background would again be suppressed substantially by this requirement as figure 5 amply suggests. Also suppressed, to an extent, would be the $WZjj$ background, whereas the $Whjj$ one would be largely unaffected.

Since, for the $t\bar{t}$ events, the invariant mass M_{jjb} constructed from the two untagged jets and one of the b-jets would cluster around the top mass, we further demand that

$$\mid M_{jjb} - M_t \mid > 30\,\text{GeV} \ . \tag{4.7}$$

for each of the b-jets. Once again, this requirement would serve to reduce the $t\bar{t}$ background to an extent (see figure 5). That this peaking is not as sharp as the one for M_{jj} is understandable as this one involves measurement of three momenta and hence is subject to larger resolution effects.

At the partonic level, all the missing transverse momenta in the $t\bar{t}$ background events is due to a single neutrino born of W-decay. Thus, if we equate $p_\nu^T = p_{\text{miss}}^T$, the longitudinal component of the neutrino momentum can be obtained within a quadratic ambiguity using the constraint that the invariant mass $M_{\ell\nu} = M_W$. This allows us, then, to reconstruct the second top. To further reduce the $t\bar{t}$ background, we may then demand that the invariant mass of the $(\ell\nu b)$ combinations should not match M_t:

$$\mid M_{\ell\nu b} - M_t \mid > 30\,\text{GeV} \ . \tag{4.8}$$

JHEP08(2007)084

Parameter set ⇒	**A**	**B**	$\sigma_{\text{background}}$(fb)		
Cuts ⇓	$\sigma_{\text{sig.}}$(fb)	$\sigma_{\text{sig.}}$(fb)	$t\bar{t}$	$W^{\pm}hjj$	$W^{\pm}Zjj$
Acceptance	2.08	0.077	8930	12	35.54
$M_{jj} \notin [65, 105]$ GeV	2.04	0.077	88.36	10.1	30.02
$\mid M_{b\bar{b}} - M_h \mid < 30$ GeV	2.04	0.077	27.29	9.45	18.65
$\mid M_{jjb} - M_t \mid, \mid M_{\ell\nu b} - M_t \mid > 30$ GeV	2.03	0.077	1.26	9.41	18.57
$\not{E}_T > 200\,\text{GeV}$	1.41	0.069	$\sim \mathcal{O}(10^{-4})$	0.21	0.47
$\not{E}_T > 300\,\text{GeV}$	0.84	0.06	$\lesssim \mathcal{O}(10^{-5})$	0.043	0.11
$\not{E}_T > 400\,\text{GeV}$	0.40	0.05	$\lesssim \mathcal{O}(10^{-7})$	0.010	0.038

Table 3: The incremental effect of cuts on the signal and background rates for the process $pp \to Q_H\bar{Q}_H \to q\bar{q}W_H^{\pm}Z_H \to b\bar{b}jj + \ell^{\pm} + \not{E}_T$. The LHT parameters are as in table 2 and have been defined in table 1. The b-tagging efficiency has been included.

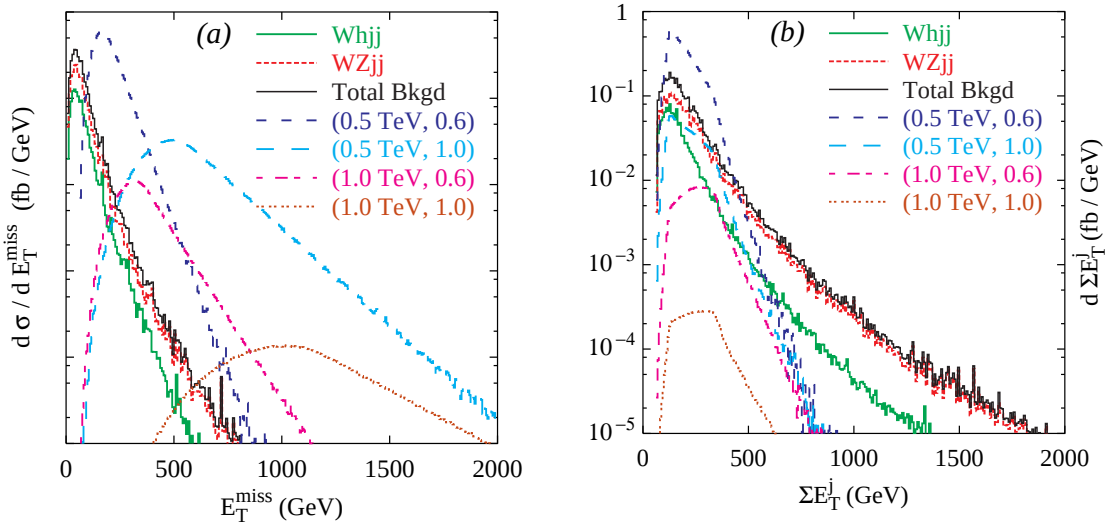

Figure 6: *(a)* Missing E_T distribution for the $jjb\bar{b}\ell^{\pm} + \not{E}_T$ final state. *(b)* Distribution in scalar sum of the two non-b jet transverse energies. Shown are the two dominant SM backgrounds as well as the signal for 4 representative points in the (f, κ) parameter space.

As table 3 shows, the imposition of the selection criteria of eqs. (4.5)–(4.8) results in suppressing the $t\bar{t}$ background by a factor $\gtrsim 7000$ while leaving the signal size essentially unaltered. Also reduced significantly is the $W^{\pm}Zjj$ background, whereas the $W^{\pm}hjj$ suffers only a minor reduction. However, owing to their large initial sizes, they still dominate the signal over the entire LHT parameter space. Indeed, as even a cursory comparison of figures 5 shows, for $m_{Q_H} \lesssim 1400\,\text{GeV}$, the sensitivity, at this stage, is background-limited rather than signal-limited. This, then, motivates the introduction of further selection cuts, and once again we consider the missing transverse momentum as well as $\sum E_T^j$, the scalar sum of the transverse energies of the two non-b jets.

As figure 6 shows, the background $\not{E}_T$ distribution is much softer in this case (as

JHEP08(2007)084

compared to that in figure 4 for the signal considered previously). This is understandable as the final state now has only one neutrino rather than the two for the previous case. And while the corresponding distributions for the signal events are softer too (again due the decrease in the number of neutrinos), the reduction is not severe. This, in part, is due to the fact that a large part of $\not{E}_T$ accrues on account of the the two (heavy) A_H's. The difference in the small $\not{E}_T$ end of the spectrum is attributable to the fact that, for the $(jj + \ell^+\ell^- + \not{E}_T)$ case, the requirement on a minimum transverse momenta for both the leptons generically implies a larger $\not{E}_T$ as well. In all, thus, the imposition of an identical cut on $\not{E}_T$ serves to improve the signal to background ratio for the $(jj+b\bar{b}+\ell^\pm+\not{E}_T)$ signal to a much larger degree than was the case for the $(jj + \ell^+\ell^- + \not{E}_T)$ one. The quantitative effect can be gauged by a perusal of table 3. Of particular interest is the fact that the ordinarily dominating $t\bar{t}$ can be eliminated to the extent of less than one event satisfying the selection criteria during the entire planned run of the LHC.

While the distribution in $\sum E_T^j$ continues to be less discriminatory than the one in $\not{E}_T$ (see figure 6), an examination of the same is, nevertheless, quite instructive. Naively, for the signal events, one would have expected this distribution to look very similar for the $(jj + \ell^+\ell^- + \not{E}_T)$ and $(jj + b\bar{b} + \ell^\pm + \not{E}_T)$ cases, since the jets are occasioned in both cases by the decay of the Q_H to a SM quark and a W_H or Z_H (with the bosons being very close in mass). That the spectra look a little different is attributable to the effect of the kinematical cuts which, of course, are different in the two cases. Once again, the distribution for the background is softer in the present case as compared to the previous one. As figure 6 suggests, it would be profitable to exploit a combination of cuts on $\not{E}_T$ and $\sum E_T^j$, so as to improve the signal to background ratio, but given the rather sharp improvement from a consideration of $\not{E}_T$ alone, we desist from doing this.

5. Discovery limit

Having established that a suitable choice of selection criteria can serve to suppress the admittedly large SM background, thereby enhancing the signal profile (for at least some parameter choices studied above), we now examine the extent to which this can be done. As a comparative study of figure 4 and figure 6 immediately shows, the $(jj+b\bar{b}+\ell^\pm+\not{E}_T)$ final state is expected to have a far better signal to noise ratio than the $(jj + \ell^+\ell^- + \not{E}_T)$ one. We may thus safely concentrate on the former in our efforts to delineate the parameter space.

In figure 7(a), we present constant cross section contours for the same. Since the requirement of $\not{E}_T > 400\,\mathrm{GeV}$ eliminates virtually all of the background (vide table 3), we have chosen to impose this. As is expected, for much of the parameter space, the cross section is primarily a function of the combination $(\kappa\, f)$ alone. At low κ and low f though, the smallness of A_H mass results in a suppression of the total missing transverse energy and hence to a relatively larger loss due to the cut on $\not{E}_T$. Similarly, the smallness of the masses of the other T-odd particles $(Q_H, W_H^\pm, Z_H)$ results in the daughter particles having smaller energies leading to a loss on account of the other selection cuts.

JHEP08(2007)084

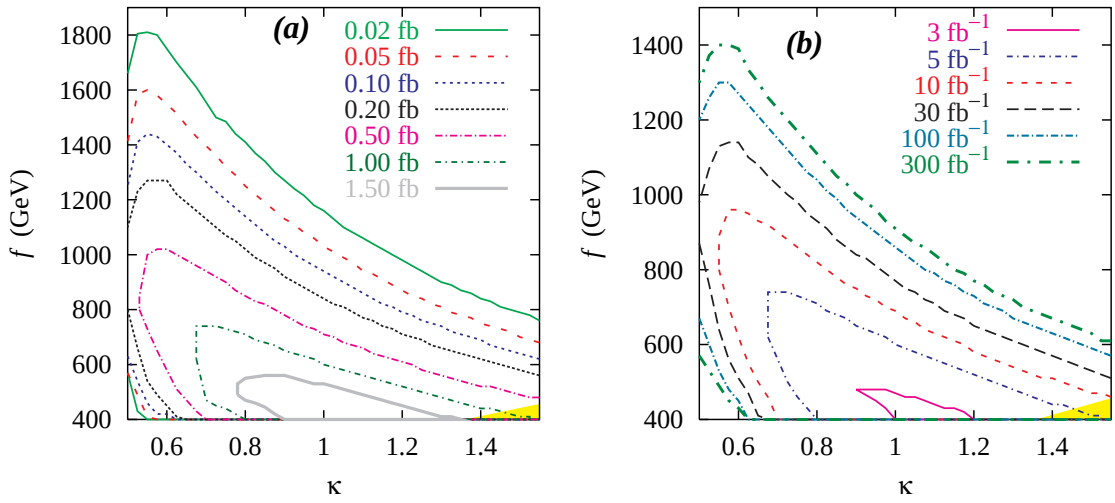

Figure 7: *(a)* Constant cross section contours in the κ-f plane for the $(jj + b\bar{b} + \ell^{\pm} + \not{E}_T)$ final state. Apart from the acceptance cuts (eqs. 4.1–4.3), the selection cuts of eqs. (4.5–4.8) and a further requirement of $\not{E}_T > 400\,\text{GeV}$ have been imposed. *(b)* The associated 5σ $(1 - \text{C.L.} = 5.7 \times 10^{-7})$ contours for different values of the integrated luminosity. The shaded region in either diagram is ruled out from the experimental requirement on the heavy quark mass [8].

This, then, reinforces the argument of the previous section in favour of either mass-dependent selection cuts or the comparison of multivariate event distributions for both signal and background (a la unbinned likelihood analysis). However, bearing in mind the nature of this analysis, we deliberately choose not to adopt such sophisticated tools and restrict ourselves to just the set of mass-dependent selection cuts mentioned above. This, of course, amounts to a conservative choice. Since both the signal and background events are small in number, we estimate the discovery limit in the LHT parameter space, assuming that they follow the well known Poisson distribution. Thus, a 5σ discovery corresponds to $1 - \alpha \leq 5.7 \times 10^{-7}$, with $\alpha(N_0)$ being the Poisson probability for seeing upto N_0 events when N_b background events are expected. In figure 7 (b) we show the 5σ discovery region in the LHT parameter space by using the signal topology of $jj + b\bar{b} + \ell^{\pm} + \not{E}_T$. As figure 7$(b)$ amply exhibits, even with a single year of low-luminosity run ($L = 10$ fb^{-1}), a remarkable part of the LHT parameter space can be probed. For the highest luminosity, the reach can be further improved, with f being probed all the way upto 1.4 TeV for $\kappa = 0.6$, while κ can be probed upto 1.5 for $f \sim 600\,\text{GeV}$. Conversely, for optimistic values of the parameters, a discovery can be made with only a few months running time.

6. Conclusions

In this paper, we have discussed two types of signatures of the first two generations of heavy T-odd quarks predicted by the Littlest Higgs model (LHT). It has been shown that T-odd heavy quarks can be copiously pair produced $(Q_H \bar{Q}_H)$ at the LHC as long as their masses

JHEP08(2007)084

are not too large [11, 10, 12]. As the heavy quarks corresponding to the first two generations are nearly degenerate (section 3), and lead to very similar final state configurations, we summed over all four flavours. In our numerical analysis, we have used the CTEQ5L parton distribution functions [18]. Whereas the production cross section depends only on the mass of the heavy quark, and hence on the product κf, both the branching fractions as well as the decay distributions have additional dependence on the scale f as we have discussed in sections 2 and 3. Once these heavy T-odd quarks are produced they will promptly decay into (T-even) standard model quarks and T-odd heavy gauge bosons ($W_H^{\pm}, Z_H, A_H$) with appropriate branching ratios which depends upon the scale f and κ as we have shown in figure 2.

We mainly focussed on the following two types of signal configurations, viz. (a) $pp \to Q_H\bar{Q}_H \to q'\bar{q}' + W_H^+W_H^- \to jj + \ell^+\ell^- + \not{E}_T$ and (b) $pp \to Q_H\bar{Q}_H \to q'\bar{q} + W_H^{\pm}Z_H \to jj + b\bar{b} + \ell^{\pm} + \not{E}_T$. The major background for the signal type (a) comes from the standard model processes $t\bar{t}$ and W^+W^-jj, whereas the standard model processes $t\bar{t}$, W^+hjj and $W^{\pm}Zjj$ comprise the major backgrounds for the signal type (b).

To estimate the number of signal and background events as well as their phase space distribution(s), we have used a parton level Monte-Carlo event generator. At first, we forced both signal as well as background events to satisfy acceptance criteria as discussed in section 4. We have then selected two sets of LHT parameters as displayed in table 1 for the purpose of comparing differential distributions as well as total cross-sections of signal and background events. It was found that the standard model background rates were order of magnitude higher than that of the signal events even after satisfying our acceptance and preliminary selection cuts. Hence, additional set of selection cuts were required to improve the signal rates. After studying distributions of different kinematic variables, we find that the missing transverse energy ($\not{E}_T$) would provide a good discriminator. As figure 4 shows, even after a stringent cut on $\not{E}_T > 400\,\text{GeV}$, signal ($a$) can supersede the background only for a small range of LHT parameters. However, for signal (b), we find a rather encouraging situation, as all three standard model background rates turn out to be significantly smaller than the signal rates once we impose the cut $\not{E}_T > 400\,\text{GeV}$ as shown in the table 3. Consequently, $pp \to Q_H\bar{Q}_H \to q'\bar{q} + W_H^{\pm}Z_H \to jj + b\bar{b} + \ell^{\pm} + \not{E}_T$ constitutes the dominant discovery channel for the first two generation T-odd heavy quarks at the LHC. Using this particular channel we have obtained 5σ discovery limit in the LHT parameter space. As figure 7(b) amply shows, adopting this methodology would allow us to make a discovery over a significant area in the allowed parameter space with only a few months' worth of data. For higher luminosities, the LHT scale f can be probed all the way upto $\sim \mathcal{O}$ (TeV) using this $jj + b\bar{b} + \ell^{\pm} + \not{E}_T$ channel. We, thus, expect that the parton level study presented in this paper will encourage the CMS and ATLAS collaboration to carry out further investigations of the Littlest Higgs Model with T-parity.

It is worthwhile to point out here that the signals considered here could potentially be mimicked by the production and subsequent decay of supersymmetric partners. For example, the final state of our decay channel (a) can arise from the production of a pair of squarks followed by their decay into charginos and then onto the lightest supersymmetric particle. Final state (b) presumably can rise from decays involving more cascades. As

JHEP08(2007)084

for the production cross section, were the gluino to be very massive, the rates for squark pair-production would typically be much smaller than those for our case. However, a relatively lighter gluino (a particle that has no analogue in the simplest LHT models) can enhance supersymmetric cross sections, both by being produced (either in pairs, or in association with a squark) and decaying into squarks, or by enhancing squark production directly through presence in the t-channel. Thus, signal (a) might be quite insufficient to distinguish LHT from supersymmetric models. The situation, though, is very different for signal (b), which though not the dominant channel, leads, nonetheless, to a better signal to background ratio. The very profile of this channel, e.g., the existence of a clearly recognisable intermediate Higgs state make it a distinctive one. Such a final state configuration is very unlikely in scenarios with a well-motivated supersymmetry breaking mechanism, and consequently, it could form a means to distinguish LHT models from supersymmetric ones.

Acknowledgments

The authors acknowledge several useful discussions with Satyaki Bhattacharya and Sukanta Dutta. DC acknowledges support from the Department of Science and Technology, India under project number: SR/S2/RFHEP-05/2006.

References

[1] Particle Data Group collaboration, S. Eidelman et al., *Review of particle physics*, *Phys. Lett.* **B 592** (2004) 1.

[2] LEP Higgs working group for Higgs boson searches, OPAL, ALEPH, DELPHI, L3 collaboration, *Search for the standard model Higgs boson at LEP*, *Phys. Lett.* **B 565** (2003) 61 [hep-ex/0306033].

[3] LEP Electroweak Working Group, online at http://lepewwg.web.cern.ch/LEPEWWG/.

[4] N. Arkani-Hamed, A.G. Cohen and H. Georgi, *Electroweak symmetry breaking from dimensional deconstruction*, *Phys. Lett.* **B 513** (2001) 232 [hep-ph/0105239];
for reviews, see, for example, M. Schmaltz and D. Tucker-Smith, *Little Higgs review Ann. Rev. Nucl. Part. Sci.* **55** (2005) 229;
M. Perelstein, *Little Higgs models and their phenomenology*, *Prog. Part. Nucl. Phys.* **58** (2007) 247 [hep-ph/0512128] and references therein.

[5] C. Csáki, J. Hubisz, G.D. Kribs, P. Meade and J. Terning, *Big corrections from a little Higgs*, *Phys. Rev.* **D 67** (2003) 115002 [hep-ph/0211124];
J.L. Hewett, F.J. Petriello and T.G. Rizzo, *Constraining the Littlest Higgs*, *JHEP* **10** (2003) 062 [hep-ph/0211218];
C. Csáki, J. Hubisz, G.D. Kribs, P. Meade and J. Terning, *Variations of little Higgs models and their electroweak constraints*, *Phys. Rev.* **D 68** (2003) 035009 [hep-ph/0303236];
M.-C. Chen and S. Dawson, *One-loop radiative corrections to the ρ parameter in the littlest Higgs model*, *Phys. Rev.* **D 70** (2004) 015003 [hep-ph/0311032];
W. Kilian and J. Reuter, *The low-energy structure of little Higgs models*, *Phys. Rev.* **D 70** (2004) 015004 [hep-ph/0311095];
Z. Han and W. Skiba, *Effective theory analysis of precision electroweak data*, *Phys. Rev.* **D 71** (2005) 075009 [hep-ph/0412166].

[6] I. Low, *T parity and the Littlest Higgs*, *JHEP* **10** (2004) 067 [hep-ph/0409025].

[7] J. Hubisz and P. Meade, *Phenomenology of the Littlest Higgs with T-parity*, *Phys. Rev.* **D 71** (2005) 035016 [hep-ph/0411264].

[8] J. Hubisz, P. Meade, A. Noble and M. Perelstein, *Electroweak precision constraints on the Littlest Higgs model with T parity*, *JHEP* **01** (2006) 135 [hep-ph/0506042].

[9] H.-C. Cheng and I. Low, *TeV symmetry and the little hierarchy problem*, *JHEP* **09** (2003) 051 [hep-ph/0308199]; *Little hierarchy, little higgses and a little symmetry*, *JHEP* **08** (2004) 061 [hep-ph/0405243].

[10] A. Freitas and D. Wyler, *Phenomenology of mirror fermions in the Littlest Higgs model with T-parity*, *JHEP* **11** (2006) 061 [hep-ph/0609103].

[11] A. Belyaev, C.-R. Chen, K. Tobe and C.P. Yuan, *Phenomenology of littlest Higgs model with T-parity: including effects of T-odd fermions*, *Phys. Rev.* **D 74** (2006) 115020 [hep-ph/0609179].

[12] M. Carena, J. Hubisz, M. Perelstein and P. Verdier, *Collider signature of T-quarks*, *Phys. Rev.* **D 75** (2007) 091701 [hep-ph/0610156].

[13] C.-S. Chen, K. Cheung and T.-C. Yuan, *Novel collider signature for little Higgs dark matter models*, *Phys. Lett.* **B 644** (2007) 158 [hep-ph/0605314].

[14] M. Asano, S. Matsumoto, N. Okada and Y. Okada, *Cosmic positron signature from dark matter in the littlest Higgs model with T-parity*, *Phys. Rev.* **D 75** (2007) 063506 [hep-ph/0602157];
A. Birkedal, A. Noble, M. Perelstein and A. Spray, *Little Higgs dark matter*, *Phys. Rev.* **D 74** (2006) 035002 [hep-ph/0603077].

[15] R.S. Hundi, B. Mukhopadhyaya and A. Nyffeler, *Invisible Higgs boson decay in the Littlest Higgs model with T-parity*, *Phys. Lett.* **B 649** (2007) 280 [hep-ph/0611116].

[16] J. Hubisz, S.J. Lee and G. Paz, *The flavor of a little Higgs with T-parity*, *JHEP* **06** (2006) 041 [hep-ph/0512169].

[17] M. Blanke et al., *Particle antiparticle mixing, ϵ_k, $\Delta\Gamma_q$, $a_{\rm SL}(q)$, $a_{CP}(B_d \to \psi K_s)$, $a_{CP}(B_s \to \psi\phi)$ and $B \to X_{s,d}\gamma$ in the littlest Higgs model with T-parity*, *JHEP* **12** (2006) 003 [hep-ph/0605214]; *Another look at the flavour structure of the littlest Higgs model with T-parity*, *Phys. Lett.* **B 646** (2007) 253 [hep-ph/0609284];

[18] CTEQ collaboration, H.L. Lai et al., *Global QCD analysis of parton structure of the nucleon: CTEQ5 parton distributions*, *Eur. Phys. J.* **C 12** (2000) 375 [hep-ph/9903282].

[19] T. Stelzer and W.F. Long, *Automatic generation of tree level helicity amplitudes*, *Comput. Phys. Commun.* **81** (1994) 357.

JHEP08(2007)084